ELSEVIER

Atmospheric Research 76 (2005) 355–376

ATMOSPHERIC RESEARCH

www.elsevier.com/locate/atmos

Triggered-lightning properties inferred from measured currents and very close electric fields

V. Kodali, V.A. Rakov*, M.A. Uman, K.J. Rambo, G.H. Schnetzer, J. Schoene, J. Jerauld

Department of Electrical and Computer Engineering, University of Florida, 553 Engineering Bldg. #33, P.O. Box 116130, Gainesville, FL 32611, United States

Received 31 October 2003; accepted 16 November 2004

Abstract

Triggered-lightning properties, including dart-leader charge density, return-stroke propagation speed, dart-leader electric potential, dart-leader propagation speed, and dart-leader current, inferred from return-stroke current and very close electric field measurements, are presented. Although most of the estimates are based on relatively crude models, they are all generally in good agreement with independent measurements and/or theoretical considerations found in the literature. The results are likely to be applicable to subsequent strokes in natural lightning.

Keywords: Lightning; Electric field; Current; Dart leader; Return stroke; Charge density; Propagation speed; Electric potential

1. Introduction

We use electric field measurements at 15 and 30 m and associated channel-base current measurements for rocket-triggered lightning (e.g., Rakov et al., 1998) to infer various properties of lightning discharges, including (1) dart-leader charge density, (2)

* Corresponding author. Tel.: +1 352 392 4242; fax: +1 352 392 8381.
E-mail address: rakov@ece.ufl.edu (V.A. Rakov).

0169-8095/$ - see front matter
doi:10.1016/j.atmosres.2004.11.036

return-stroke propagation speed, (3) dart-leader electric potential, (4) dart-leader propagation speed, and (5) dart-leader current. The measurements were made at the International Center for Lightning Research and Testing (ICLRT) at Camp Blanding, Florida, during the summers of 1999, 2000, and 2001. The instrumentation and experimental set-up used at the ICLRT in these years are described in Section 2. Only those instruments used to measure quantities needed for the present study are described. Additional information on the ICLRT is found in the works of Crawford et al. (2001), Rakov et al. (2001), Uman et al. (2002), Schoene et al. (2003a,b), and Kodali (2003). Triggered-lightning strokes are similar to subsequent strokes in natural lightning (e.g., Fisher et al., 1993). Therefore, the results presented in this paper are likely to apply also to subsequent strokes in natural lightning.

2. Experiments

The ICLRT at Camp Blanding, Florida, was established in 1993 by the Electric Power Research Institute (EPRI) and Power Technologies, Inc. (PTI) to study the effects of lightning on power lines. It has been operated by the University of Florida since 1994. The rocket-and-wire technique (e.g., Rakov et al., 1998) was used to artificially initiate (trigger) lightning from natural thunderclouds. An overview of the ICLRT during the 1999, 2000, and 2001 experiments is found in Fig. 1 and a photograph of Flash S0012, triggered in 2000, in Fig. 2. Examples of measured electric field and electric field derivative ($\mathrm{d}E/\mathrm{d}t$) waveforms are shown in Fig. 3. Statistical characteristics of the electric and magnetic field waveforms and their time derivatives measured at 15 and 30 m in 1999 and 2000 are presented by Schoene et al. (2003a).

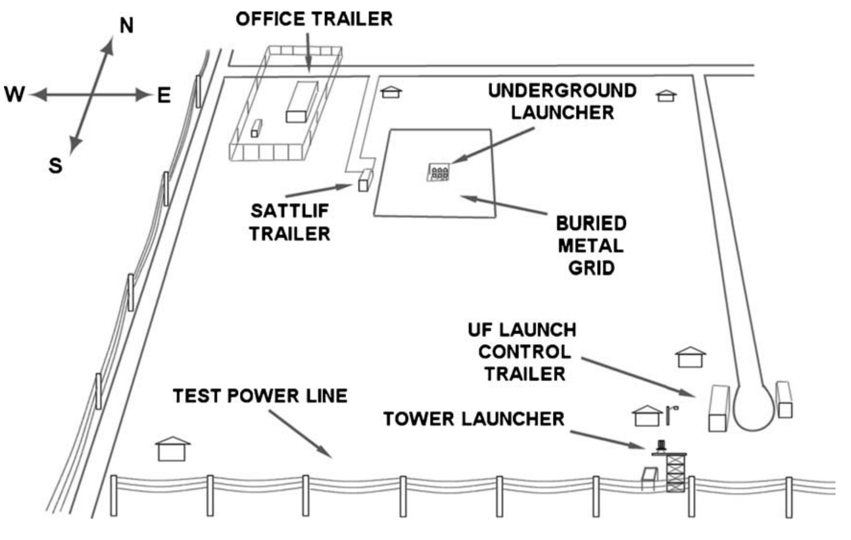

Fig. 1. An overview of the ICLRT at Camp Blanding, Florida, 1999–2001. Not all test objects are shown.

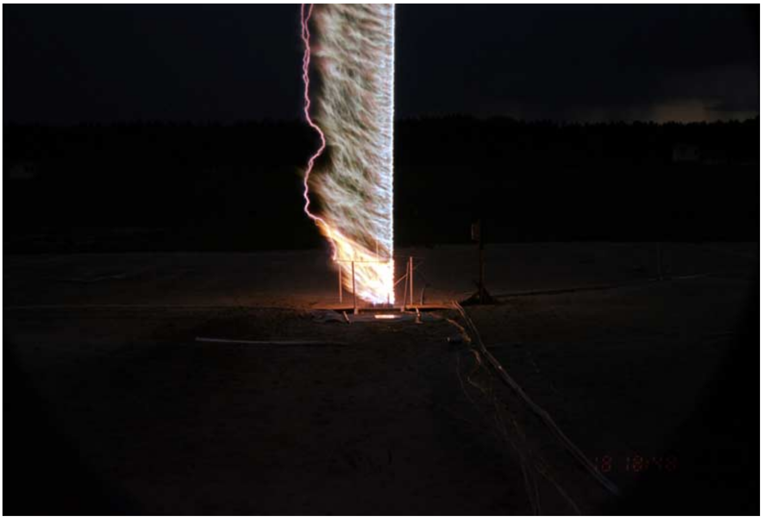

Fig. 2. Photograph of lightning flash S0012 triggered from the underground launcher (see Fig. 1).

2.1. 1999 experiment

2.1.1. General information

The rocket launcher consisted of six metallic tubes from which rockets were launched. The rocket launcher was mounted on insulating fiberglass legs and placed underground, with the top of the launcher flush with ground, in a 4 m × 4 m × 4 m pit. The pit and the launcher were located in the center of a 70 m × 70 m buried metallic grid (see Fig. 1) intended to simulate a perfectly conducting ground. This configuration eliminates ground surface arcing (e.g., Rakov et al., 1998) and minimizes field propagation effects due to a finite ground conductivity. The low frequency, low current grounding resistance of the buried grid was measured to be 6 Ω. A hollow metal rod with an outside diameter of 3.8 cm and a wall thickness of 0.6 cm protruding 1 m above the ground surface was used as the strike object for flashes S9901–S9918 in 1999. For the other flashes triggered in 1999 (flashes S9925–S9935), a 2 m rod was used in order to increase the probability of lightning attachment to the rod. During 1999, the underground launcher was connected via four metal straps to the buried grid and the base of the launcher was connected via two metal straps to a 16.5 m long vertical ground rod whose low frequency, low current grounding resistance was measured to be 40 Ω.

The electric field, magnetic field, and their time derivatives produced by lightning strokes were measured 15 and 30 m from the strike rod. A TTL-level digital pulse trigger signal was generated when the magnetic field sensor located 15 m from the rocket launcher detected a magnetic field that corresponded to a current of at least 5 kA (using Ampere's law of magnetostatics). The TTL signal was transmitted to the external trigger input of the Le Croy oscilloscopes located in the SATTLIF trailer (see Fig. 1) to trigger the digitizing system. The oscilloscopes for the field and current measurements had a pre-trigger (stored data recorded prior to the trigger pulse) that ranged from 10% to 50% of the

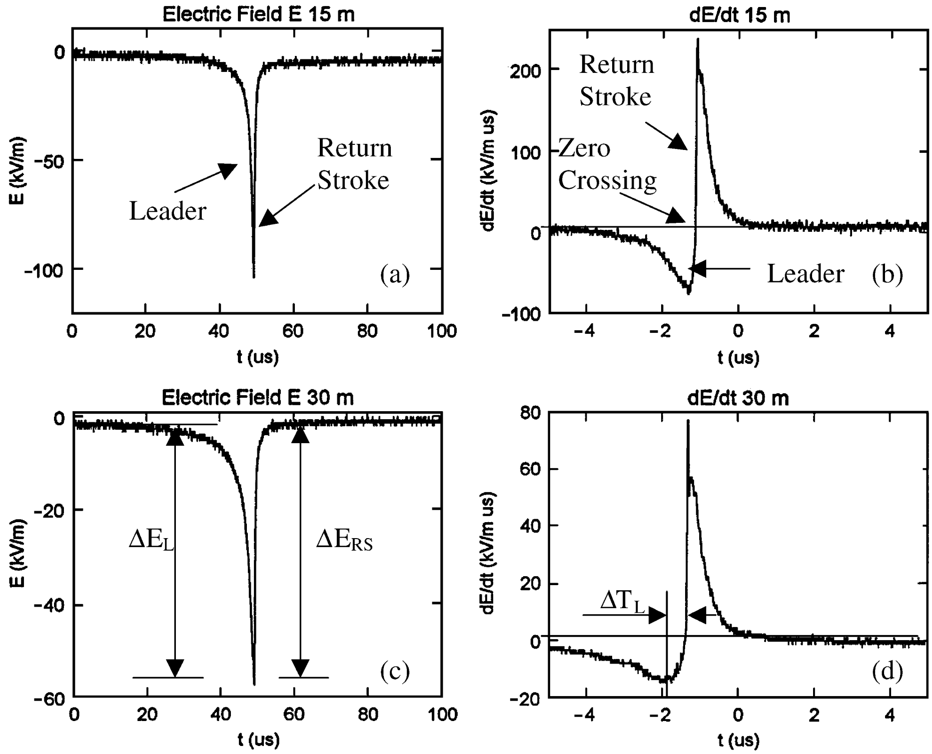

Fig. 3. Vertical electric field (E) and electric field derivative ($\mathrm{d}E/\mathrm{d}t$) waveforms for stroke 2 in rocket-triggered flash S9918 measured 15 and 30 m from the lightning channel at Camp Blanding, Florida. (a) Electric field at 15 m, (b) Electric field derivative at 15 m, (c) Electric field at 30 m showing leader (ΔE_L) and return stroke (ΔE_{RS}) field changes, used in estimating the leader charge density (Section 3) and return stroke speed (Section 4), and (d) Electric field derivative at 30 m showing measurement of the time interval ΔT_L between the leader $\mathrm{d}E/\mathrm{d}t$ peak and the $\mathrm{d}E/\mathrm{d}t$ zero crossing. This time interval from records at 15 m was used in estimating the dart leader speed (see Section 6).

total record length. Fiber optic transmitters (FOT) converted the analog output signals from the antennas to optical signals and transmitted those signals via fiber optic cables to fiber optic receivers (FOR). Meret and Nanofast fiber optic links (FOL) were used in the experiment. The bandwidth of the Meret and Nanofast FOLs was dc to 35 MHz and 5 Hz to 175 MHz, respectively. The FOTs were powered with 12 V dc lead-acid batteries. RG-58 or RG-223 coaxial cables (both 50 Ω) connected the FOT to the antennas. The FORs in the SATTLIF trailer were powered with 120 V ac uninterruptible power supplies (UPS). RG-58 or RG-223 coaxial cables connected the FOR to the digitizing system. The optical fibers transmitting the signal from the FOT to the FOR were 200 μm glass, Kevlar-reinforced, duplex cables. The oscilloscopes had 8-bit amplitude resolution.

2.1.2. Instrumentation for current measurements

Six P110A current transformers (CTs) with a lower frequency response of 1 Hz and an upper frequency response of 20 MHz were used to measure the current at the lightning channel base, two measured the current flow to the vertical ground rod, and four measured the current flow to the buried grid. The current amplitude range of each sensor is from a few amperes to approximately 20 kA. A passive combiner summed the two signals from the ground rod CTs to obtain a total ground rod current, and another one summed the four signals from the buried grid CTs to obtain a total grid current. The total ground rod current signal and the total grid current signal were then each transmitted via separate Meret FOL (35 MHz bandwidth) to the SATTLIF trailer. Both signals were filtered with a 20 MHz, −3 dB anti-aliasing filters and then digitized at 50 MHz (20-ns sampling interval). The total current at the lightning channel base was obtained by numerically summing the ground-rod current and the buried-grid current. Most of the current went to the grid.

2.1.3. Instrumentation for electric field measurements

Electric fields were measured using flat plate antennas with an area of 0.16 m^2, placed essentially flush with the ground. The output of each electric field antenna was connected to an integrating capacitor of value 105 nF at 15 m and 55 nF at 30 m. The input impedance of the fiber optic transmitter was about 1 MΩ. Meret fiber optic links with a bandwidth of 35 MHz were used to transmit the signal to the SATTLIF trailer where the 15-m electric field signals were filtered using 10 MHz, −3 dB anti-aliasing filters and digitized at 25 MHz (40-ns sampling interval), and the 30-m electric field signals were filtered using 20 MHz, 3 dB anti-aliasing filters and digitized at 25 MHz (40-ns sampling interval). No aliasing is expected (and no evidence of it is observed) in the latter case, since the field spectrum is typically limited to less than 10 MHz.

2.1.4. Instrumentation for electric field derivative measurements

Electric field derivatives were measured using flat plate antennas with an area of 0.16 m^2. The output of each electric field derivative antenna was terminated using 50 Ω, and the input impedance of the fiber optic transmitter was about 1 MΩ. Meret fiber optic links with a bandwidth of 35 MHz were used to transmit the 15-m signal, and a Nanofast FOL was used to transmit the 30-m signal to SATTLIF trailer. Signals of dE/dt at 15 and 30 m were filtered using 20 MHz, −3 dB anti-aliasing filters and digitized at 250 MHz (4-ns sampling interval).

2.2. 2000 experiment

The strike object was a 2 m vertical rod surrounded by a 3 m diameter horizontal ring elevated to 1.5 m height and electrically connected to the base of the rod (Miki et al., 2002, Fig. 3). Most of the 2000 instrumentation was the same as the 1999 instrumentation except for the two major changes made in 2000 and listed below: (1) The triggering signal was generated when the current measured at the strike rod base exceeded 3 kA. (2) Current at the channel base was measured simultaneously by two different methods (a) the total lightning current was measured using a single current viewing resistor (upper frequency response 8 MHz) installed just below the strike object (new measurement), and (b) the current components flowing to the vertical ground rod and to the buried grid were measured individually and added numerically to obtain the total lightning current. The current to the ground rod was measured as in 1999, while the currents to the buried grid were measured with two current viewing resistors in the two connections rather than with the four current transformers and four connections used in 1999. The strike-object current signal was transmitted via Nicolet Isobe fiber optic link (dc to 14 MHz bandwidth) to the SATTLIF trailer where it was digitized at 50 MHz (20-ns sampling interval). Electric field and electric field derivative instrumentation in 2000 was the same as in 1999.

2.3. 2001 experiment

The experimental set-up was the same as in 2000, except for the strike ring and the ground rod connection were removed. Additionally, the 2 m strike rod was replaced with 4.5 m section of gas pipeline for the experiments on August 18, 2001. The pipeline was mounted directly onto the current viewing resistor, and nylon fishing line was used to support the structure. The pipeline consisted of four sections of different diameters, the sections being connected by three different insulating joints. The insulating joints were bridged by electric arcs produced by lightning strokes. Strike-object current was measured in the same way as in 2000, but was digitized at 25 MHz (40-ns sampling interval), instead of 50 MHz (20-ns sampling interval) as in 2000. The electric field and electric field derivative instrumentation in 2001 was the same as in 1999 and 2000.

3. Leader charge density

The overall electric field change, relative to the background electric field due to cloud charges, for a vertical, uniformly charged leader above a perfectly conducting ground (see Fig. 4) is given by (e.g., Uman, 1987, Appendix A)

$$\Delta E_{\mathrm{L}} = \frac{\rho_{\mathrm{L}}}{2\pi\varepsilon_0 r}\left[\frac{1}{\left(1+z_t^2/r^2\right)^{1/2}} - \frac{1}{\left(1+H_m^2/r^2\right)^{1/2}} - \frac{(H_m - z_t)H_m}{r^2\left(1+H_m^2/r^2\right)^{3/2}}\right] \tag{1}$$

where ρ_{L} is the line charge density along the leader channel, $\varepsilon_0 = 8.85 \times 10^{-12} F/m$, r is the horizontal distance from the ground strike point (prospective point of leader termination on the ground) to an observation point P, H_m is the height of the cloud charge, equal to the height of the top of the leader channel, $z_t = H_m - v_{\mathrm{L}} t$ is the height of the descending leader tip above ground at time t, where v_{L} is the leader speed. As shown by Rubinstein et al. (1995), if $z_t = 0$ (a fully developed leader channel) and $H_m \gg 2r$ (an observation point P on the ground very close to the leader channel termination point), the vertical electric field change ΔE_{L} due to a uniformly charged leader can be expressed as

$$\Delta E_{\mathrm{L}} = \rho_{\mathrm{L}}/(2\pi\varepsilon_0 r). \tag{2}$$

Note that the leader electric field change (ΔE_{L}) is often referred to as the leader electric field (E_{L}) for brevity.

Crawford et al. (2001) inferred, from multiple-station electric field measurements within some hundreds of meters of the lightning channel, a more or less uniform distribution of charge along the bottom kilometer or so of the dart-leader channel in rocket-

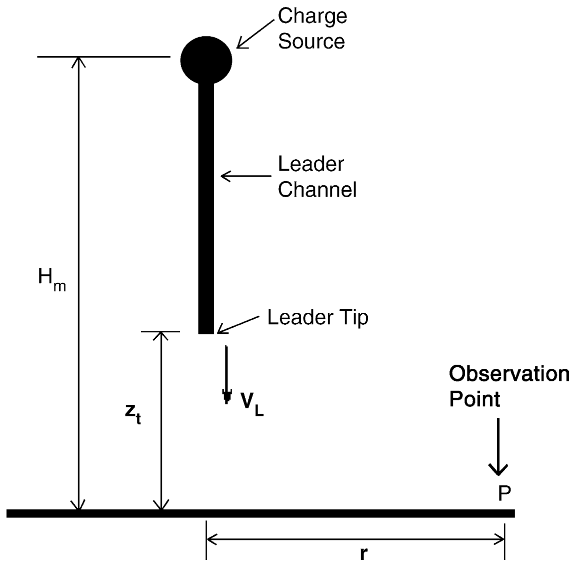

Fig. 4. The geometry used in deriving Eq. (1).

triggered lightning. This observation simply indicates that for such a relatively short channel section a non-uniform charge density distribution will appear approximately uniform. Cooray et al. (2004) compared Crawford et al.'s (2001) experimental results with theoretical predictions for a vertical conductor in an external electric field and found a fairly good agreement. It is worth noting that the contribution to ΔE_{L} from upward connecting leaders, if any, is expected to be negligible. For example, Rubinstein et al. (1995) estimated that the contribution to the total electric field change at 30 m from charges residing at heights less than 5 m above ground (a uniform charge density distribution was assumed) is only 3%.

We use values of ΔE_{L} measured at $r=15$ m and $r=30$ m at the ICLRT in 1999–2001 and Eq. (2) to estimate the corresponding values of ρ_{L}. The results are presented in Fig. 5a and b. For all data combined, the mean values of ρ_L from the electric field measurements at 15 and 30 m are 98 and 101 μC/m, respectively. The overall range of variation is from 26 to 210 μC/m. The inferred values of ρ_{L} are used in Section 5 below for estimating the electric potential of dart-leader channel and in Section 6 for estimating the leader propagation speed.

4. Return-stroke propagation speed

For the transmission line (TL) model (Uman and Mclain, 1969), the longitudinal current $I(z',t)$ in a straight and vertical channel at any height z' and any time t is given by (Fig. 6)

$$I(z',t) = I(0, t - z'/v_{\mathrm{RS}}) \tag{3}$$

where $I(0,t)$ is the current at the channel base ($z'=0$), and v_{RS} is the return stroke propagation speed assumed to be constant. The associated line charge density on the

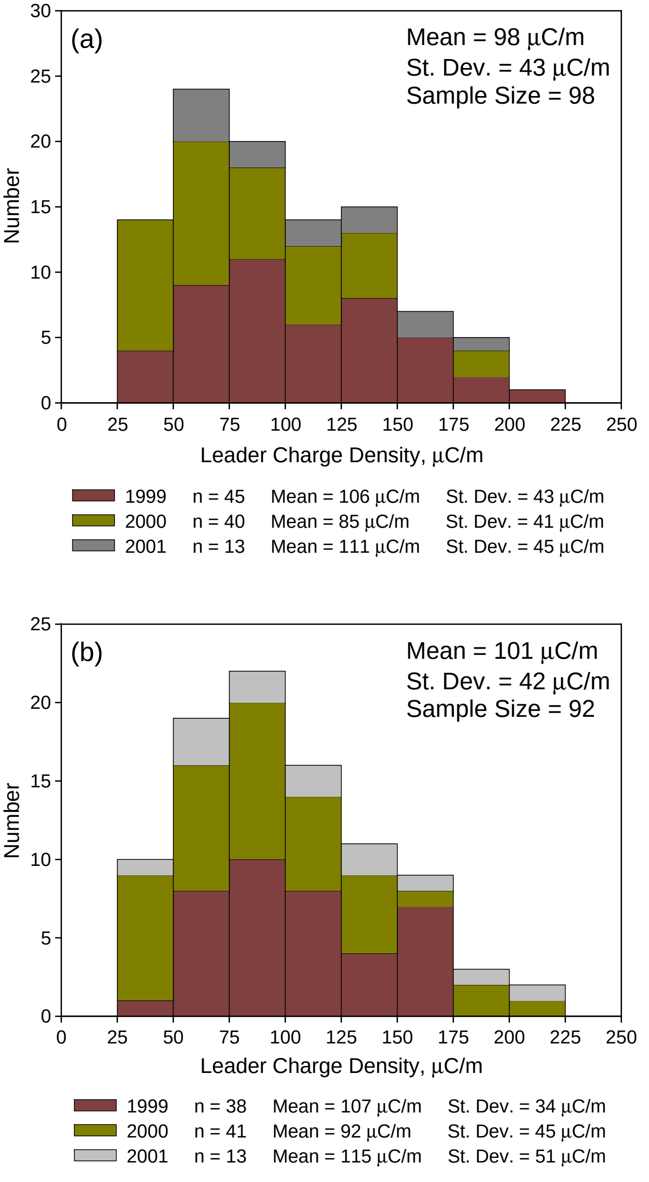

Fig. 5. Dart-leader line charge density inferred from measurements of electric fields at (a) 15 m and (b) 30 m at the ICLRT in 1999, 2000, and 2001.

channel can be expressed, using the current continuity equation, as (Thottappillil et al., 1997)

$$\rho_{\mathrm{RS}}(z', t) = \frac{I(0, t - z'/v_{\mathrm{RS}})}{v_{\mathrm{RS}}}. \tag{4}$$

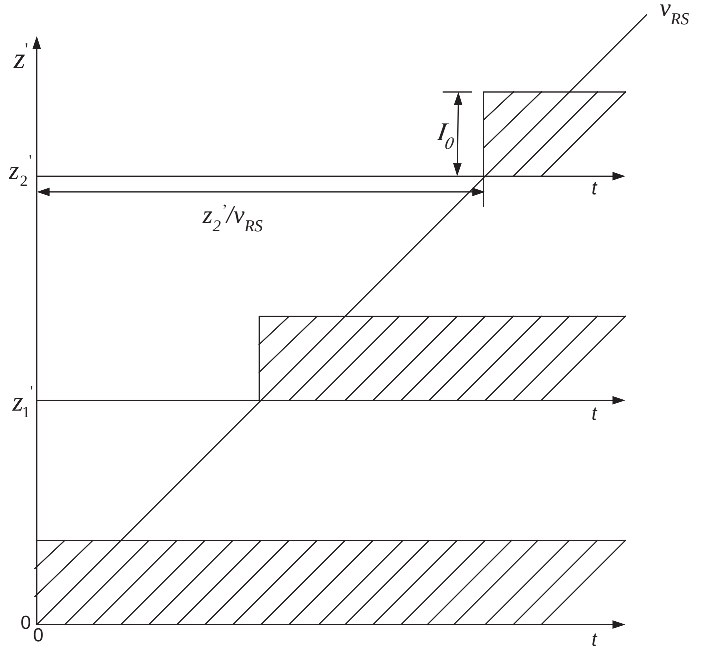

Fig. 6. Illustration of the transmission line model (Uman and Mclain, 1969). Shaded step-function waveforms represent current as a function of time at ground ($z'=0$) and at two heights z_1' and z_2' above ground. Current at the lightning channel base ($z'=0$) is specified as $I(0,t)=I_0u(t)$ where $u(t)$ is the Heaviside function equal to unity for $t \geq 0$ and zero otherwise. The slanted line represents the return-stroke propagation speed v_{RS}.

If the channel-base current is assumed to be a step function of magnitude I_0, that is,

$$I(z', t) = I_0 u(t - z'/v_{RS}) \tag{5}$$

then

$$v_{RS} = \frac{I_0}{\rho_{RS}}. \tag{6}$$

The line charge density along the return-stroke channel can be found from the measured close electric field change ΔE_{RS} due to the return stroke as (Thottappillil et al., 1997)

$$\rho_{RS} = 2\pi\varepsilon_0 r \Delta E_{RS} \tag{7}$$

We obtained estimates of the return-stroke speed using Eqs. (6) and (7) and assuming that I_0 is approximately equal to the return-stroke peak current, which was determined from measured current waveforms. Since Eq. (6) is valid only when the return-stroke current is a step-function wave propagating along the channel at a constant speed, our speed values are very rough estimates. The results are shown in Fig. 7a and b. For all

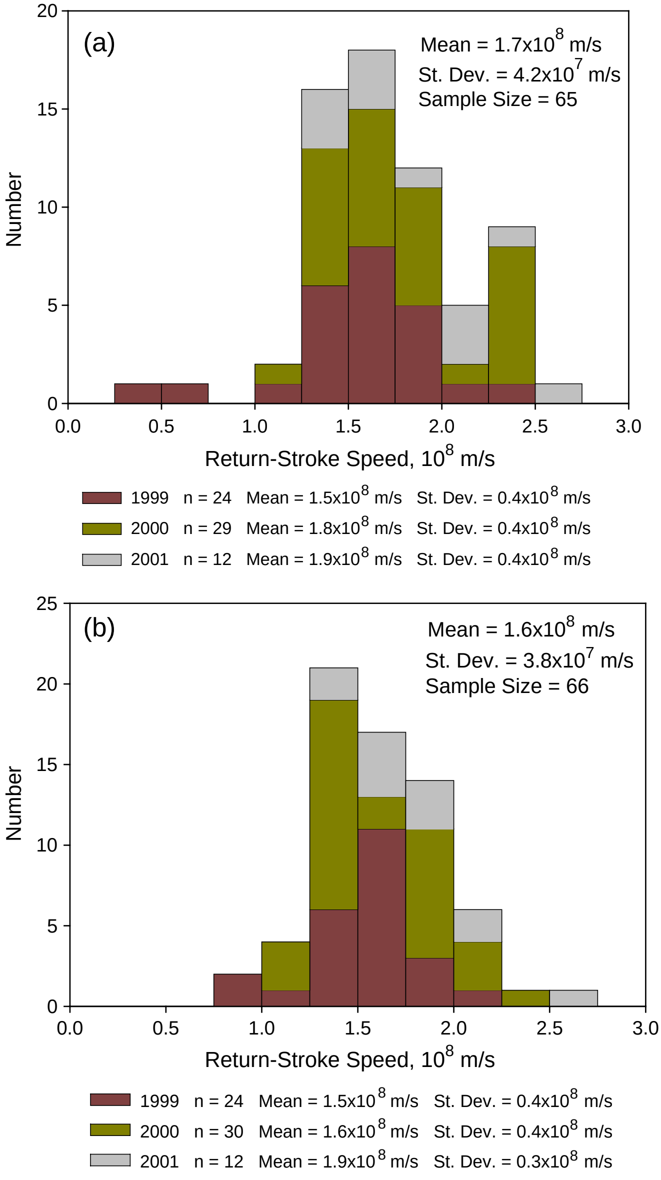

Fig. 7. Return-stroke speed inferred from measurements of electric fields at (a) 15 and (b) 30 m and channel-base currents at the ICLRT in 1999, 2000, and 2001.

data combined, the mean values estimated using electric field measurements at 15 and 30 m are 1.7×10^8 and 1.6×10^8 m/s, respectively. The overall range of variation is from about 3×10^7 to 2.7×10^8 m/s. The estimated speed values are consistent with optical measurements found in the literature (see Rakov et al., 1992 for a review).

5. Dart-leader electric potential

The electric potential, V, of the lightning dart leader channel can be estimated as

$$V = \rho_L / C \tag{8}$$

where ρ_L is the line charge density on the leader channel, assumed to be constant for the bottom kilometer or so (see Section 3), and C is the capacitance per unit length of the channel. Values of ρ_L for the bottom kilometer or so of the lightning channel were computed from measured close leader electric field changes, as discussed in Section 3, and C is taken from Bazelyan et al. (1978) as

$$C = \frac{2\pi\varepsilon_0}{\ln(2h/a)}. \tag{9}$$

In Eq. (9), a is the radius of the leader channel, and h is the height above ground. It is assumed in deriving Eq. (9) that $h \gg a$, but this condition can be relaxed by replacing

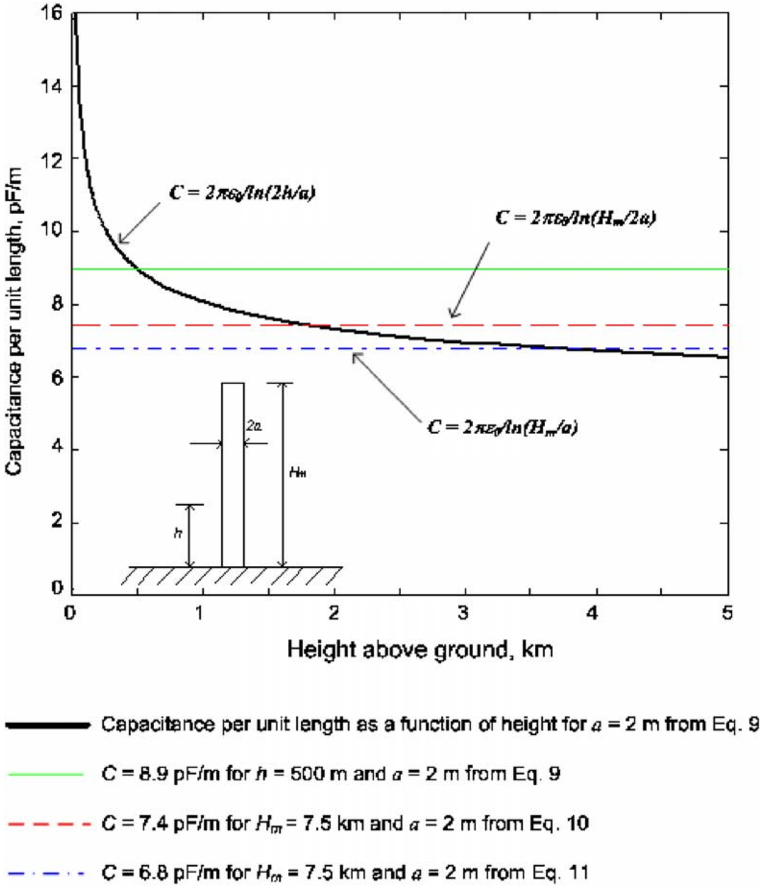

Fig. 8. Capacitance per unit length vs. height h above ground given by Eq. (9) where channel radius a is set at 2 m. The horizontal solid, dashed, and dot-dashed lines indicate values of capacitance per unit length estimated from Eq. (9) (h=500 m, a= 2 m), Eq. (10) (H_m=7.5 km, a= 2 m), and Eq. (11) (H_m=7.5 km, a= 2 m), respectively.

$\ln(2h/a)$ by $\cosh^{-1}(h/a)$. Clearly, C decreases with increasing h (see Fig. 8), although the variation at relatively large heights is rather slow. In using Eq. (9), we assumed that $a = 2$ m (taking into account the radial corona sheath surrounding the channel core and containing the bulk of the leader charge) and that $h = 500$ m (midpoint of the bottom kilometer of the channel considered here). The assumed value of a is consistent with Gauss' Law, if the

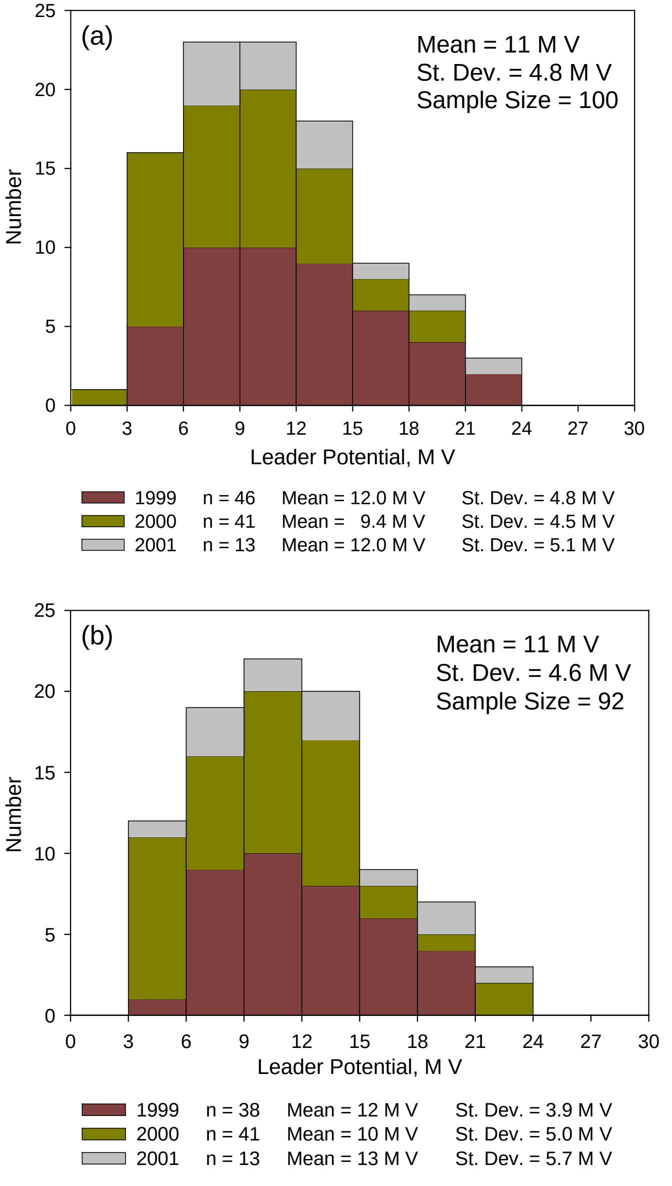

Fig. 9. Dart-leader potential inferred from measurements of electric fields at (a) 15 m and (b) 30 m at the ICLRT in 1999, 2000, and 2001.

line charge density and breakdown electric field in the warm air previously conditioned by the initial-stage current and possibly by preceding leader/return-stroke sequences are assumed to be 100 μC/m and 1 MV/m, respectively. The resultant value of C is 8.9 pF/m (see the horizontal solid line in Fig. 8). It is worth noting that C is a relatively insensitive function of a, varying (at h=500 m) from 4.8 to 10.5 pF/m as a varies from 1 cm to 5 m. In this simplified approach, the leader channel potential is proportional to the measured leader electric field change. The results are presented in Fig. 9. For all data combined, the mean value of leader potential, corresponding to the bottom kilometer or so (to a height of 500 m, at which C is computed, to be exact) is 11 MV, the same for 15-m and 30-m electric field measurements, with the overall range of variation being from about 3 to 24 MV. The estimated values of electric potential are consistent with the 15 MV value previously inferred for subsequent strokes by Rakov (1998).

A similar approach to estimating the potential of stepped leaders in natural lightning was used by Mazur and Ruhnke (2002, 2003), although they employed the average capacitance per unit length, expressed as a function of the total channel height, H_m,

$$C = \frac{2\pi\varepsilon_0}{\ln(H_m/2a)}. \tag{10}$$

Using their equation and assuming that H_m=7.5 km (expected for Florida), we compute C=7.4 pF/m (horizontal dashed line in Fig. 8). A slightly different equation for the average capacitance per unit length,

$$C = \frac{2\pi\varepsilon_0}{\ln(H_m/a)} \tag{11}$$

is given by Berger (1977). This latter formula yields 6.8 pF/m (horizontal dot-dashed line in Fig. 8). Our capacitance estimate, 8.9 pF/m, is within about 25% of the values given by Eqs. (10) and (11).

6. Dart-leader propagation speed

For a uniformly charged leader (Fig. 4), one can find from electrostatic considerations the height z_t=H of the descending leader tip above ground at the time of maximum dE/dt, as shown below. The starting point is Eq. (1) with the last term representing the source at height H_m above ground ($H_m \gg z_t$, $H_m \gg r$) neglected,

$$E_\mathrm{L} = \frac{\rho_\mathrm{L}}{2\pi\varepsilon_0 r}\left[\frac{1}{\left(1+z_t^2/r^2\right)^{1/2}} - \frac{1}{\left(1+H_m^2/r^2\right)^{1/2}}\right] \tag{12}$$

where $z_t = H_m - v_\mathrm{L} t$.

The corresponding equation for the leader electric field derivative with respect to time is,

$$\frac{\mathrm{d}E_\mathrm{L}}{\mathrm{d}t} = \frac{\rho_\mathrm{L} v_\mathrm{L}}{2\pi\varepsilon_0 r^3}\,\frac{z_t}{\left(1+z_t^2/r^2\right)^{3/2}} \tag{13}$$

Differentiating $\mathrm{d}E_\mathrm{L}/\mathrm{d}t$ with respect to time and equating the result to zero, we obtain

$$\frac{\rho_\mathrm{L} v_\mathrm{L}}{2\pi\varepsilon_0 r^3} \frac{1 - 2z_t^2/r}{\left(1 + z_t^2/r^2\right)^{5/2}} = 0. \tag{14}$$

Solving Eq. (14) for $z_t = H$, we get

$$H = r/\sqrt{2} \tag{15}$$

which is the height of the leader tip above ground at the time of maximum leader $\mathrm{d}E/\mathrm{d}t$. It appears that at a given r, the maximum $\mathrm{d}E/\mathrm{d}t$ is a measure of leader current $I_\mathrm{L} = \rho_\mathrm{L} v_\mathrm{L}$ (see Section 7 below).

The value of leader speed was estimated from Eq. (13) using (1) the measured value of negative maximum leader $\mathrm{d}E/\mathrm{d}t$, (2) $z_t = r/\sqrt{2}$, and (3) the value of ρ_L found from measured electric field in Section 3. We used only dart-leader $\mathrm{d}E/\mathrm{d}t$ signatures recorded at $r = 15$ m, since such signatures at $r = 30$ m were generally unpronounced (the 30-m $\mathrm{d}E/\mathrm{d}t$ signature in Fig. 3d, showing a well pronounced leader part, is one of a few exceptional cases). The results are shown in Fig. 10. The range of dart-leader speed variation is from 1.1×10^7 to 7.3×10^7 m/s, with the mean value being 3.5×10^7 m/s. This mean value of speed is about a factor of two higher than the mean value of dart-leader speed, 1.6×10^7 m/s, reported from optical measurements for triggered lightning by Jordan et al. (1992).

For alternatively estimating the leader speed one can also use the value of H (Eq. (15)) and the time required for the leader to propagate from height H to ground that is equal to the time interval ΔT_L between the leader $\mathrm{d}E/\mathrm{d}t$ peak and the $\mathrm{d}E/\mathrm{d}t$ zero crossing (see Fig.

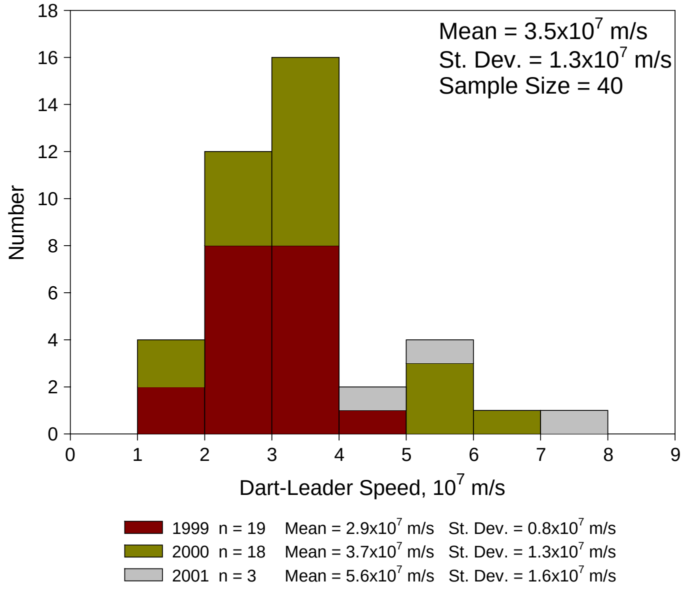

Fig. 10. Dart-leader speed inferred from maximum leader $\mathrm{d}E/\mathrm{d}t$ and leader electric field measured at 15 m at the ICLRT in 1999, 2000, and 2001.

3d). We measured ΔT_L from dE/dt records at 15 m and then computed leader speeds as $v_L = H/\Delta T_L$, where H=11 m (from Eq. (15)). For all data combined, the mean value of dart-leader speed is 7.5×10^7 m/s, about a factor of two higher than that estimated using the first method (Fig. 10), with the overall range of variation being from 2.0×10^7 to 1.5×10^8 m/s. These values of inferred dart-leader speed are near the upper end of the range based on optical measurements (the highest measured value is 4.9×10^7 m/s; Jordan et al., 1992) or in the range of return-stroke speeds (e.g., Rakov et al., 1992). The reason for the discrepancy between these latter speed estimates (the average speed within the bottom 11 m of the channel) and the results shown in Fig. 10 (the value of speed at a height of 11 m above ground) is unclear. Highly resolved optical measurements of the dart-leader speed at the final stages of its development are needed for understanding this discrepancy.

7. Dart-leader current

Dart-leader current, $I_L = \rho_L v_L$ was estimated from Eq. (13) using (1) the measured value of maximum leader dE/dt, $(\mathrm{d}E/\mathrm{d}t)_{\max}$, and (2) $z_t = r/\sqrt{2}$,

$$I_L = kr^2(\mathrm{d}E/\mathrm{d}t)_{\max} \tag{16}$$

where $k = \left(\sqrt{3}\right)^3 \pi\varepsilon_0$=144.5 pF/m.

Dart-leader currents were estimated from $(\mathrm{d}E/\mathrm{d}t)_{\max}$ values measured at 15 m. The results are presented in Fig. 11. The overall range of variation is from 1 to 11 kA, with the

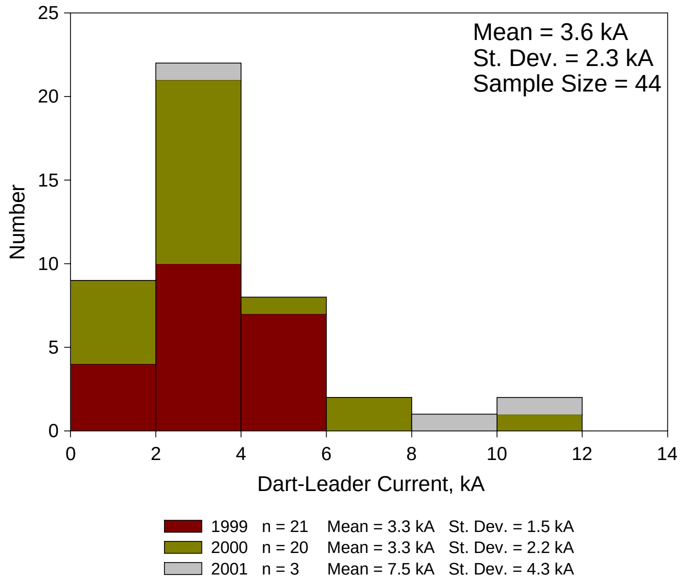

Fig. 11. Dart-leader current inferred from measurements of maximum leader dE/dt at 15 m at the ICLRT in 1999, 2000, and 2001.

mean values being 3.6 kA. The corresponding mean ratio of dart-leader to return-stroke current is 0.22 (the range of variation from 0.12 to 0.85).

Idone and Orville (1985) estimated dart-leader peak currents for 22 leaders in two rocket-triggered lightning flashes using two different optical techniques. In method (1), the ratio of the dart-leader and return-stroke currents was taken as equal to the ratio of the dart-leader and return-stroke speeds; this assumes a simple model in which an equal charge per unit length is involved in each process. The speed ratio and the return-stroke

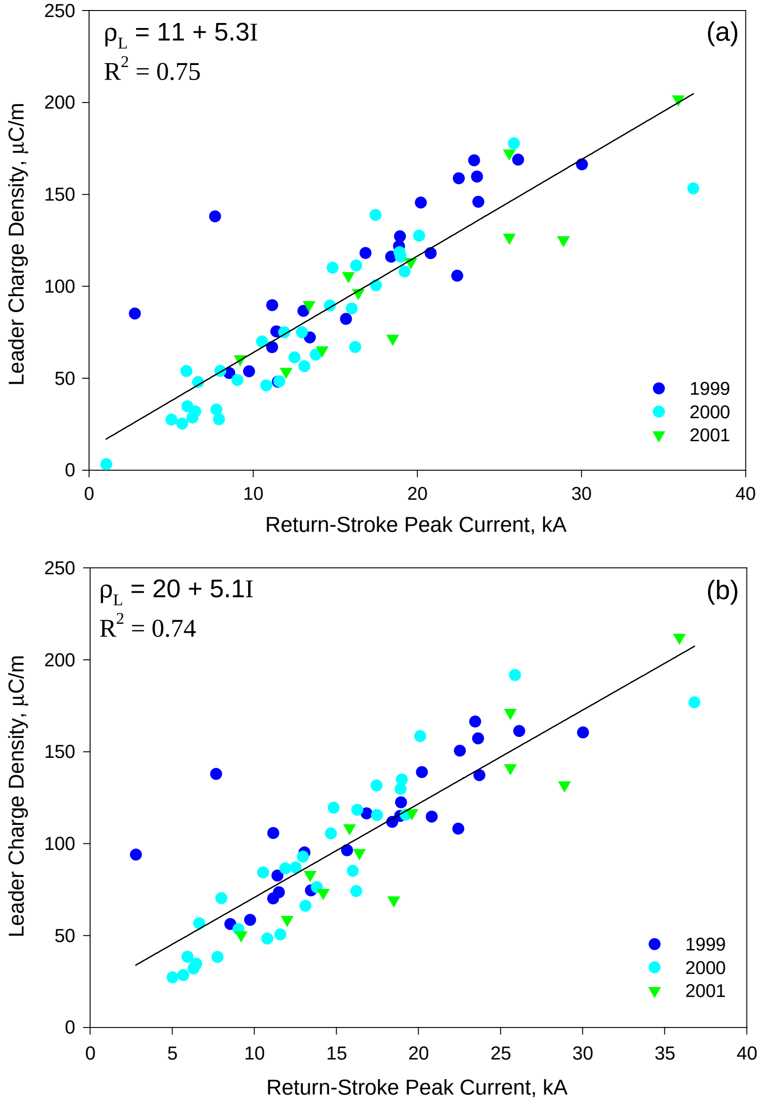

Fig. 12. Dart-leader line charge density calculated from leader electric field change measured at (a) 15 m and (b) 30 m vs. return-stroke peak current.

current were measured, allowing a calculation of the dart-leader current. In method (2) the relation between return-stroke peak current I_R and return-stroke peak relative light intensity L_R in each of two flashes studied by Idone and Orville (1985) ($L_R=1.5I_R^{1.6}$ and $L_R=6.4I_R^{1.1}$) was applied to the dart-leader relative light intensity in that flash to determine the dart-leader current. The two techniques produced very similar results, a mean current of 1.8 kA for method (2) and 1.6 kA for method (1). Individual values

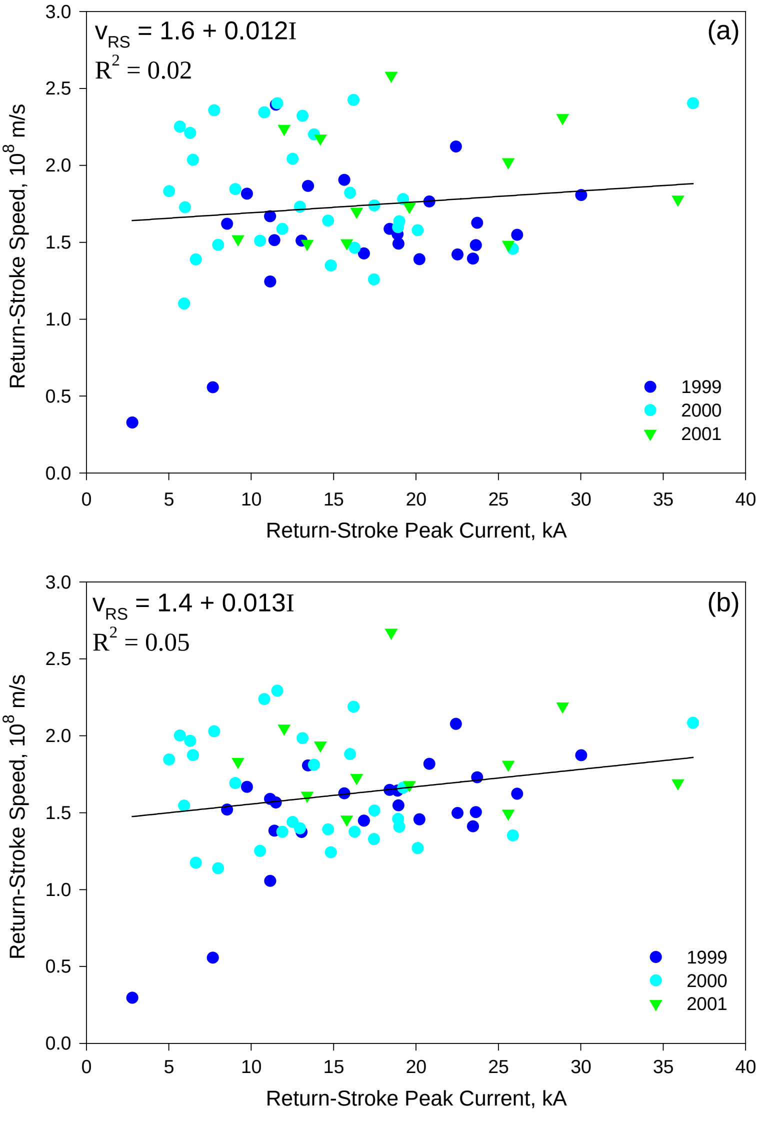

Fig. 13. Return-stroke speed calculated from return-stroke electric field change measured at (a) 15 m and (b) 30 m and peak current measured at the channel base vs. return-stroke peak current.

ranged from 100 A to 6 kA. The ratio of dart-leader to return-stroke current ranged from 0.03 to 0.3 with a mean of 0.17 from method (2) and 0.16 from method (1). The largest dart-leader to return-stroke current ratios were associated with the largest return-stroke currents and relative light intensities. Our estimates of dart-leader current and of the ratio of dart-leader to return-stroke current are in fairly good (given the assumptions involved) agreement with those of Idone and Orville (1985), 3.6 kA vs. 1.6–1.8 kA and 0.22 vs.

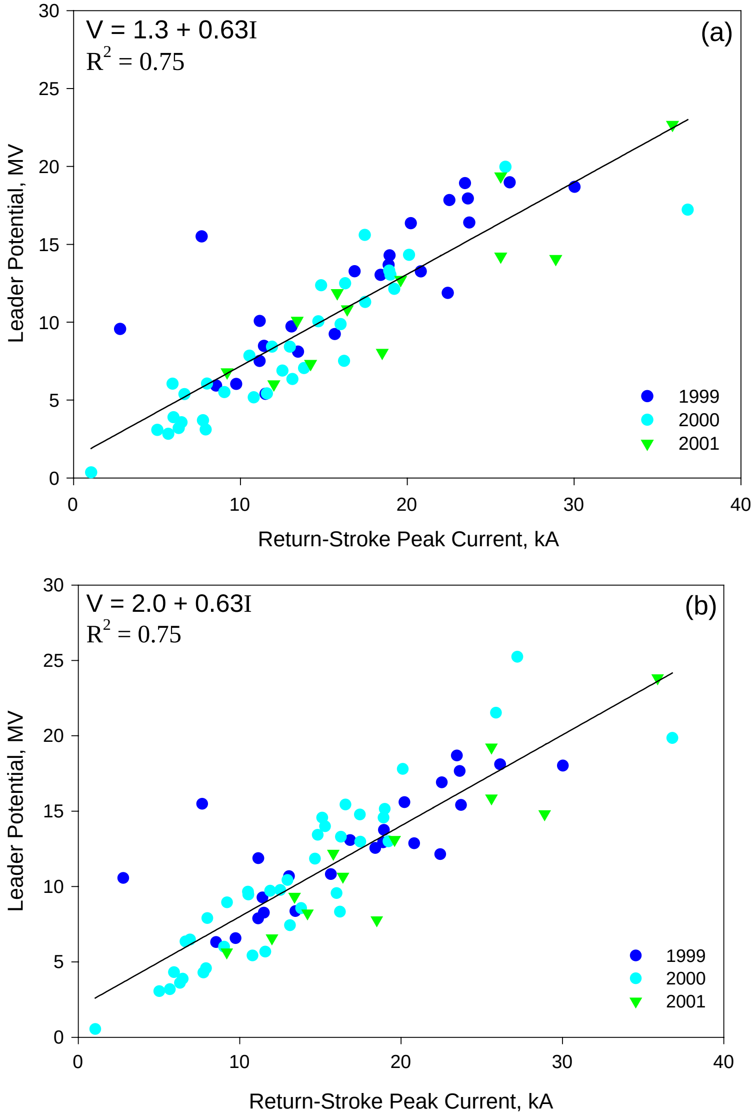

Fig. 14. Electric potential of the dart-leader channel calculated from leader electric field change measured at (a) 15 m and (b) 30 m vs. return-stroke peak current.

0.16–0.17, respectively, although we did not observe a clear tendency for the largest ratios to be associated with the largest return-stroke currents (see Section 8).

8. Correlation between parameters

Figs. 12–16 are scatter plots of lightning properties including inferred dart-leader charge density, return-stroke speed, dart-leader potential, dart-leader speed, and dart-leader current vs. measured peak current for 1999, 2000, and 2001. From these plots, leader charge density (Fig. 12), leader potential (Fig. 14), and leader current (Fig. 16) exhibit a linear correlation with peak current. It is worth noting that in the simple models used here the leader charge density and leader electric potential are proportional to the leader electric field change, and the latter is known to be strongly correlated with the return-stroke peak current (Rubinstein et al., 1995; Rakov et al., 1998; Miki et al., 2002). From Figs. 13 and 15, the return stroke speed and dart-leader speed show essentially no dependence on return-stroke peak current.

Willett et al. (1989) and Mach and Rust (1989) found a lack of correlation between the optically measured return-stroke propagation speed and the return-stroke peak current in triggered lightning. Idone et al. (1984) did observe “a nonlinear relationship” between these two parameters in triggered lightning, but it disappears if one excludes the relatively small events that are characterized by return-stroke peak currents less than 6–7 kA, in order to make the sample of Idone et al. (1984) similar to those of Willett et al. (1989) and Mach and Rust (1989). If there was a relationship between the return-stroke speed and

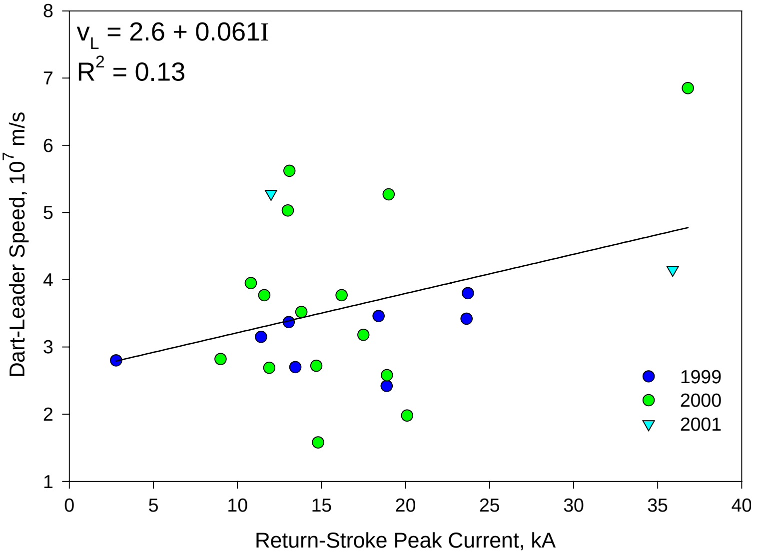

Fig. 15. Dart-leader speed calculated from maximum leader dE/dt and leader electric field measured at 15 m vs. return-stroke peak current.

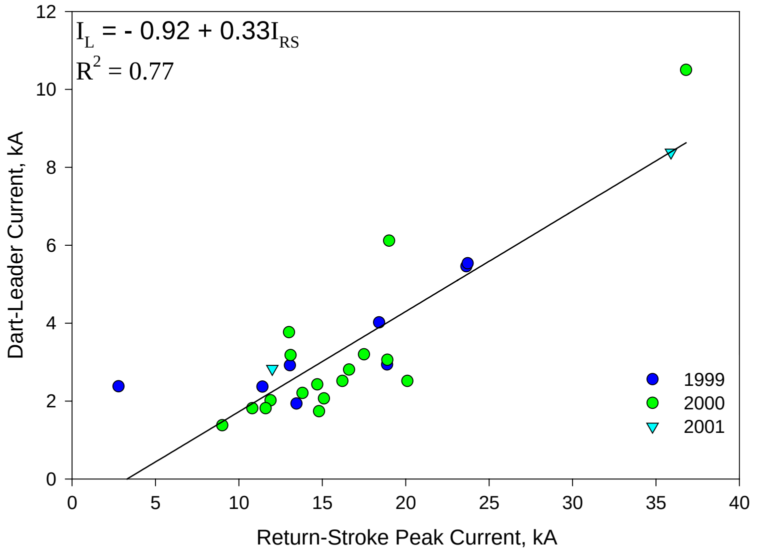

Fig. 16. Dart-leader current calculated from maximum leader dE/dt measured at 15 m vs. return-stroke peak current.

return-stroke current, as might be expected on physical grounds, then it would be influenced by many factors and, as a result, characterized by a large scatter. Our results are consistent with those of Willett et al. (1989) and Mach and Rust (1989). On the other hand, our results for the dart-leader speed shown in Fig. 15 appear to be inconsistent with those of Jordan et al. (1992) who examined correlation between the optically measured dart-leader speed (averaged over some hundreds of meters of the channel) and return-stroke peak current. They reported correlation coefficients of +0.84 and +0.73 for rocket-triggered lightning in New Mexico and Florida, respectively, versus +0.36 in our Fig. 15 (note that the determination coefficient, R^2, given in Fig. 15 is the square of the correlation coefficient, R).

9. Summary

The estimates of dart-leader charge density, return-stroke propagation speed, dart-leader electric potential, dart-leader propagation speed, and dart-leader current are generally in reasonably good agreement with independent measurements and/or theoretical considerations found in the literature. Our results suggest that for a typical triggered-lightning return stroke, the dart-leader line charge density is about 100 μC/m, the return-stroke speed is about two-thirds of the speed of light, the dart-leader potential is about 11 MV, the dart-leader speed 11 m above ground is 3.5×10^7 m/s, and the dart-leader current is a few kiloamperes. In the data set used for examining the dart-leader speed and dart-leader current the mean return-stroke peak current was between 16 and 17 kA, and for all other inferred parameters it was between 15 and 16 kA. Since these values of return-stroke peak current are close to those expected for subsequent strokes in natural lightning, the parameters of rocket-triggered lightning strokes given above are likely to apply also to subsequent strokes in natural lightning.

Acknowledgment

This work was supported in part by NSF grants ATM-9726100, ATM-0003994, and ATM-0346164, and DOT (FAA) grant 99-G-043. L. Ruhnke and D. Wang provided comments on this paper. W. Tuni helped with Fig. 8.

References

Bazelyan, E.M., Gorin, B.N., Levitov, V.I., 1978. Physical and Engineering Foundations of Lightning Protection. Gidrometeoizdat, Leningrad, USSR.

Berger, K., 1977. The Earth flash. In: Golde, R.H. (Ed.), Lightning, Physics of Lightning, vol. 1. Academic Press, New York, pp. 119–190.

Cooray, V., Rakov, V., Theethayi, N., 2004. The relationship between the leader charge and the return stroke current-Berger's data revisited. Proc. of the 27th Int. Conf. on Lightning Protection, Avignon, France.

Crawford, D.E., Rakov, V.A., Uman, M.A., Schnetzer, G.H., Rambo, K.J., Stapleton, M.V., Fisher, R.J., 2001. The close lightning electromagnetic environment: dart-leader electric field change versus distance. J. Geophys. Res. 106, 14909–14917.

Fisher, R.J., Schnetzer, G.H., Thottappillil, R., Rakov, V.A., Uman, M.A., Goldberg, J.D., 1993. Parameters of triggered lightning flashes in Florida and Alabama. J. Geophys. Res. 98, 22887–22902.

Idone, V.P., Orville, R.E., 1985. Correlated peak relative light intensity and peak current in triggered lightning subsequent return strokes. J. Geophys. Res. 90, 6159–6164.

Idone, V.P., Orville, R.E., Hubert, P., Barret, L., Eybert-Berard, A., 1984. Correlated observations of three triggered lightning flashes. J. Geophys. Res. 89, 1385–1394.

Jordan, D.M., Idone, V.P., Rakov, V.A., Uman, M.A., Beasley, W.H., Jurenka, H., 1992. Observed dart leader speed in natural and triggered lightning. J. Geophys. Res. 97, 9951–9957.

Kodali, V., 2003. Characterization of Close Lightning Electromagnetic Fields. Masters Thesis, University of Florida.

Mach, D.M., Rust, W.D., 1989. Photoelectric return-stroke velocity and peak current estimates in natural and triggered lightning. J. Geophys. Res. 94, 13237–13247.

Mazur, V., Ruhnke, L.H., 2002. Determining leader potential in cloud-to-ground flashes. Geophys. Res. Lett. 29 (12). doi:10.1029/2001GL014159.

Mazur, V., Ruhnke, L.H., 2003. Determining the striking distance of lightning through its relationship to leader potential. J. Geophys. Res. 108 (D14), 4409. doi:10.1029/2002JD003047.

Miki, M., Rakov, V.A., Rambo, K.J., Schnetzer, G.H., Uman, M.A., 2002. Electric fields near triggered lightning channels measured with Pockels sensors. J. Geophys. Res. 107 (D16). doi:10.1029/2001JD001087.

Rakov, V.A., 1998. Some inferences on the propagation mechanisms of dart leaders and return strokes. J. Geophys. Res. 103, 1879–1887.

Rakov, V.A., Thottappillil, R., Uman, M.A., 1992. On the empirical formula of Willett et al. relating lightning return stroke peak current and peak electric field. J. Geophys. Res. 97, 11527–11533.

Rakov, V.A., Uman, M.A., Rambo, K.J., Fernandez, M.I., Fisher, R.J., Schnetzer, G.H., Thottappillil, R., Eybert-Berard, A., Berlandis, J.P., Lalande, P., Bonamy, A., Laroche, P., Bondiou-Clergerie, A., 1998. New insights into lightning processes gained from triggered-lightning experiments in Florida and Alabama. J. Geophys. Res. 103, 14117–14130.

Rakov, V.A., Crawford, D.E., Rambo, K.J., Schnetzer, G.H., Uman, M.A., Thottappillil, R., 2001. M-component mode of charge transfer to ground in lightning discharges. J. Geophys. Res. 106, 22817–22831.

Rubinstein, M., Rachidi, F., Uman, M.A., Thottappillil, R., Rakov, V.A., Nucci, C.A., 1995. Characterization of vertical electric fields 500 m and 30 m from triggered lightning. J. Geophys. Res. 100, 8863–8872.

Schoene, J., Uman, M.A., Rakov, V.A., Kodali, V., Rambo, K.J., Schnetzer, G.H., 2003a. Statistical characteristics of the electric and magnetic fields and their time derivatives 15 m and 30 m from triggered lightning. J. Geophys. Res. 108 (D6), 4192. doi:10.1029/2002JD002698.

Schoene, J., Uman, M.A., Rakov, V.A., Rambo, K.J., Jerauld, J., Schnetzer, G.H., 2003b. Test of the transmission line model and the traveling current source model with triggered lightning return strokes at very close range. J. Geophys. Res. 108 (D23), 4737. doi:10.1029/2003JD003683.

Thottappillil, R., Rakov, V.A., Uman, M.A., 1997. Distribution of charge along the lightning channel: relation to remote electric and magnetic fields and to return-stroke models. J. Geophys. Res. 102, 6987–7006.

Uman, M.A., 1987. The Lightning Discharge. Academic Press, San Diego California.

Uman, M.A., McLain, D.K., 1969. Magnetic field of lightning return stroke. J. Geophys. Res. 74, 6899–6910.

Uman, M.A., Schoene, J., Rakov, V.A., Rambo, K.J., Schnetzer, G.H., 2002. Correlated time derivatives of current, electric field intensity, and magnetic flux density for triggered lightning at 15 m. J. Geophys. Res. 107 (D13) (11 pp.). doi:10.1029/2000JD000249.

Willett, J.C., Bailey, J.C., Idone, V.P., Eybert-Berard, A., Barret, L., 1989. Submicrosecond intercomparison of radiation fields and currents in triggered lightning return strokes based on the transmission-line model. J. Geophys. Res. 94, 13275–13286.